Diagnostic in CVD processes by IR pyrometry

Cyril Gasquères, Florin-Daniel Duminica, Francis Maury

Diagnostic in CVD processes by IR pyrometry

Cyrille Gasqueres, Florin-Daniel Duminica, Francis Maury *

Centre Interuniversitaire de Recherche et d'Ingénierie des Matériaux (CIRIMAT), ENSIACET 118 Route de Narbonne, 31077 Toulouse Cedex 4, France

Abstract

The control of CVD processes requires *in situ* analysis techniques and real time monitoring to identify the chemical species involved in the mechanism, to determine the growth kinetics and more generally to detect and analyze the dynamics of any event occurring during the growth of the film. We demonstrate through four representative examples that IR pyrometry allows to answer to the last two items, which make it an attractive diagnostic tool for CVD processes, simple to use, sensitive at nanometric scale, economic and being able to operate either under atmospheric or low pressure. Thus, we monitored the initial stages of the growth of conducting diffusion barriers CrC_xN_y on Si and as a second example, we have followed their heat treatment to detect possible phase transformations. The case of MOCVD of Fe reveals the high sensitivity of this diagnostic technique. Indeed, the abrupt changes of the pyrometric signal correlate remarkably to changes in the growth mode. Lastly, the characteristic oscillations due to multireflexions at the interfaces observed in the first stages of the growth of transparent TiO_2 film allow the real time determination of the growth rate. These examples show the great diagnostic potentialities of IR pyrometry for the optimization and the control of CVD processes.

Keywords: IR pyrometry; *In situ* diagnostic; CVD

1. Introduction

In addition to its first function of temperature measurement, we show in this paper through four representative examples that IR pyrometry can be used as an original diagnostic tool for CVD processes. The understanding, the data acquisition for modelling and the control of CVD processes require the implementation of several techniques, more or less sophisticated, for the *in situ* and real time analysis of: (i) the chemical species, (ii) the kinetics of growth and (iii) more generally of any event occurring during the growth of a thin film (incubation period, growth mode, transformation, etc . . .). If various methods make possible the identification of the nature of the chemical species in CVD processes as for example the optical spectroscopies, generally they cannot be used to analyze the kinetics of the surface reactions and the dynamics of the layer growth. For this goal, specific techniques are carried out like those operating under very low pressures like RHEED diffraction [1] and the near-threshold photoemission [2], or rather heavy equipments and non-trivial treatment of the data such as reflectance difference spectroscopy (RDS) [3], surface photo-absorption (SPA) [4] and p-polarized reflectance spectroscopy (PRS) [5] and to a less extent ellipsometry.

The great sensitivity of the optical pyrometry makes possible to detect the dynamics of surface phenomena during the growth of thin layers with the advantage of a particularly simple and low cost technique, working under the specific ambient of CVD processes under atmospheric pressure since low pressures are not necessary for this analysis. The IR pyrometry was used for example to study the germination of diamond [6] and to determine the growth rate in a microwaves plasma process [7–9]. It was also used during the MBE growth of partially opaque layers of III–V semiconductors [10,11]. We show in this article that it offers greater potentialities and that it can be applied in various processes and for the control of the growth of an extended variety of thin film materials.

2. Experimental

The optical bi-band pyrometers are specifically designed to measure the real temperature of the aimed objects whatever the differences in emissivity of the materials (an auto-correction being done). They are obviously powerful tools for this function covering a wide range of temperature. On the other hand,

* Corresponding author. Tel.: +33 5 62 88 56 69; fax: +33 5 62 88 56 00.
E-mail address: Francis.Maury@ensiacet.fr (F. Maury).

doi:10.1016/j.cep.2007.01.005

a basic monochromatic pyrometer will be cheaper but it will be very sensitive to the variations of emissivity of the heated body. The determination of the temperature in this case requires the knowledge and a manual correction of the emissivity coefficient. If this parameter is deliberately fixed, the detected pyrometric signal will follow the variations of emissivity of the concerned object to give an apparent temperature. These variations and their origins are exploited when the IR pyrometry is used as a diagnostic tool.

A vertical cold wall MOCVD reactor was used to deposit various films of non-oxide ceramic type (CrC_xN_y), metal (Fe) and functional oxide (TiO_2). The temperature of the substrates was measured by a thermocouple inserted into the sample-holder near to the substrate. A monochromatic IR pyrometer ($\lambda = 1.6\ \mu m$; model AOIP TR7020E) was used to monitor the radiation emitted by the substrate through the quartz wall of the reactor at an incidence of approximately 30° compared to the normal. Unless otherwise specified, the emissivity coefficient was fixed at the value of Si ($\varepsilon = 0.68$). The real time acquisition of the pyrometric signal was made on a computer.

3. IR pyrometric monitoring of CrC_xN_y films on Si

3.1. Influence of the film thickness

The CrC_xN_y layers are conducting diffusion barriers which have a metallic like aspect. Fig. 1 shows that in the early stage of the growth of CrC_xN_y on Si the apparent temperature decreases before to be stabilized after a certain time, *i.e.* a certain thickness. At the beginning, *i.e.* prior to deposition the detected radiation originates from the Si substrate, the difference between the real temperature (400 °C) and the value measured by IR pyrometry (387 °C) is explained by the incidence angle which is not normal to the surface and the passage through the reactor wall. As soon as the growth starts, the radiation emitted by the substrate is partially absorbed by the film until a critical thickness beyond which it becomes opaque. The apparent temperature is then significantly different from the real temperature due to the difference of the emissivity coefficients ε between the film and the substrate. This emissivity variation of the film–substrate couple can be modelled by taking into account the deposition rate G, the absorption coefficient α of film and spectral brightness L, as detailed elsewhere [12]:

$$L_{\lambda,T}^{\text{film/sub}} = \exp(-\alpha G t)\varepsilon_{\lambda,T}^{\text{sub}} L_{\lambda,T}^{\text{bb}} \quad (1)$$

Clearly, if α is known (which is not the case for the CrC_xN_y phase) the deposition rate could be determined in the early stages of the growth.

3.2. Control of CVD processes: detection of an interphase

Under certain CVD conditions, the decrease of the pyrometric signal is observed only after a period (t_{int}) more or less long (Fig. 2). The first assumption about this period was the existence of an incubation time. However, even after a few seconds of deposition, XPS analyses have revealed the presence of Cr, C, N and O on the substrate which discards this hypothesis. In fact, the formation of thin layer transparent to the radiation emitted by the substrate occurs in the early stages with likely an emissivity coefficient similar to the substrate. SIMS profiles clearly confirmed the formation of this oxidized interphase (Fig. 3). It is probable that this oxidized Cr-containing interphase has an emissivity coefficient close to that of Cr_2O_3 ($\varepsilon = 0.7$) which is of the same order than that of Si ($\varepsilon = 0.68$). When residual oxygen likely present on the reactor wall was consumed, the CrC_xN_y layer starts to grow and its emissivity coefficient is then related to that of Cr metal ($\varepsilon = 0.3$) inducing a significant decrease of the pyrometric signal. This interpretation is confirmed by the good agreement between the thickness of this interphase determined by SIMS and by IR pyrometry (Table 1). Indeed, this thickness can be directly measured from SIMS profiles (Fig. 3) and can also be determined from the period t_{int} measured by IR pyrometry (Fig. 2).

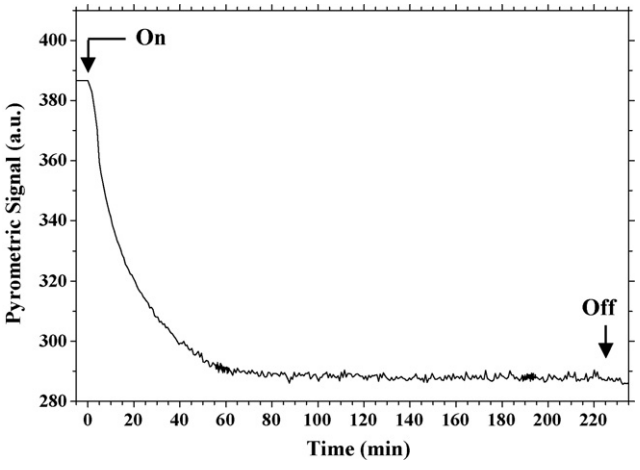

Fig. 1. Typical dependence of the pyrometric signal on the time during the growth of CrC_xN_y films on Si. The arrows indicate the starting (opening of the Cr precursor bubbler) and the end of the deposition ($T = 400$ °C; $\varepsilon = 0.68$).

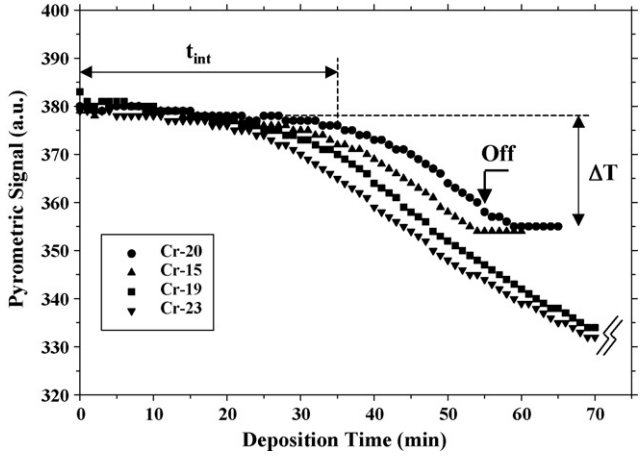

Fig. 2. Temporal variation of the pyrometric signal in the initial stages of the growth of CrC_xN_y thin films deposited on SiO_2 substrates at 400 °C ($\varepsilon = 0.68$). The parameters determined from these *in situ* analyses and reported in Table 1 (after Ref. [12]).

Table 1
Correlation between data resulting from the *in situ* analyses by optical pyrometry and *a posteriori* by SIMS showing a good agreement between the calculated thickness of oxidized interphase (t_{cal}^{int}) and experimental thickness (t_{exp}^{int})

Sample	Growth conditions			IR pyrometry		Thickness (SIMS)		
	T (°C)	Substrate	Time (min)	ΔT (°C)	t_{int} (min)	t_{exp}^{int} (nm)	t_{cal}^{int} (nm)	t_{total} (nm)
Cr23	400	SiO_2	90	64	20	21	25	71
Cr19	400	SiO_2	90	67	28	35	35	120
Cr15	400	SiO_2	50	25	32	38	40	47
Cr20	400	SiO_2	55	25	35	34	44	40
Cr22	420	SiO_2	55	36	30	51	38	56
Cr33	400	Si	190	99	7	9	9	260
Cr24	400	Si	25	5	25	23	31	23
Cr29	420	Si	35	52	3	5	4	30
Cr25	420	Si	25	3	25	26	31	26

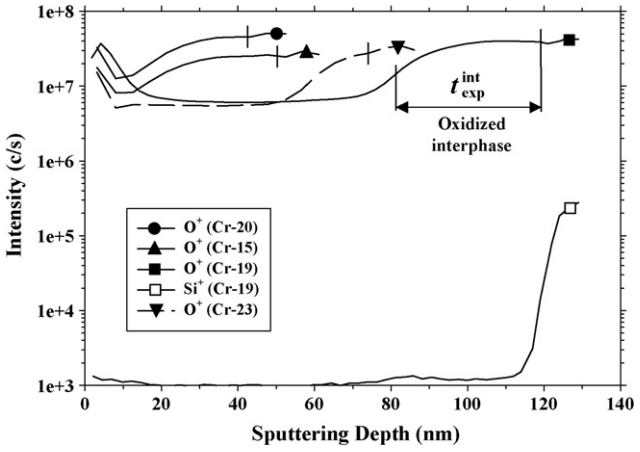

Fig. 3. SIMS depth profiles of CrC_xN_y films grown at 400 °C on SiO_2 substrates. As a result of a partial oxidation of the interface, a $CrC_xN_yO_z$ interphase is formed whose thickness depends on the CVD parameters. The film–substrate interface is indicated on the oxygen profiles by a vertical line. Only one profile of Si is shown as representative example (sample Cr19).

4. Heat treatment of $Cr_3(C,N)_2$ coatings controlled by IR pyrometry

Various heat treatments of amorphous as-deposited CrC_xN_y layers were carried out directly in the deposition reactor in order to study their thermal stability. These post-treatments were controlled *in situ* by IR pyrometry in order to detect any surface modification. During annealing either under vacuum or under H_2, the CrC_xN_y film crystallizes to form the ternary compound $Cr_3(C,N)_2$ and no variation of the pyrometric signal is observed. Structural change does not affect the emissivity of the material. Under He at 650 °C, the pyrometric signal does not change during the heat treatment for 30 min (Fig. 4a). The apparent temperature is slightly lowered compared to the real temperature because the emissivity coefficient of the film is lower than that of Si. By contrast, during annealing at 700 °C under He atmosphere, after the transition stage (2–3 min) leading to the stabilization of the true temperature (steady range), a progressive increase of the pyrometric signal occurs which is not observed under the other annealing conditions (Fig. 4b). The apparent temperature becomes approximately equal with the real temperature after about 15 min, indicating that the emissivity of the sample surface increases up to a value close to that of silicon. For this sample, the X-ray diffraction (XRD) analysis reveals the presence of chromium oxide Cr_2O_3 after annealing at 700 °C, whereas no significant change of the diffraction patterns was observed for samples annealed under He at lower temperatures (Fig. 5).

Moreover, oxidized chromium has an emissivity of about 0.7 very close to that of Si fixed on the pyrometer (0.68). The emissivity of the sample thus increases due to the surface oxidation. The oxidation being observed at the end of the heat treatment, this means that this oxide is doubtless formed on the external surface of the sample likely due to oxygen

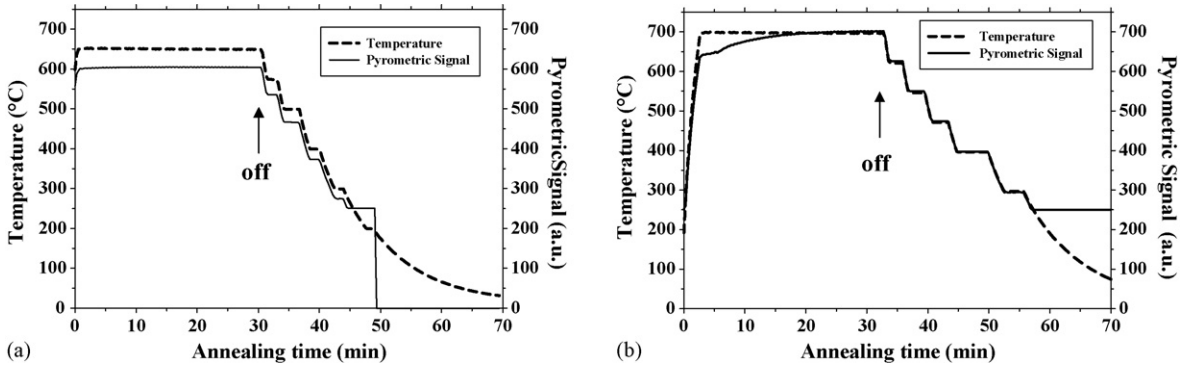

Fig. 4. Time dependence of the pyrometric signal during annealing of the $Cr_3(C,N)_2$ film under He: (a) 30 min at 650 °C; (b) 30 min at 700 °C. The emissivity was fixed at the value of silicon ($\varepsilon_{Si} = 0.68$). The arrow noted off shows when the heating is stopped.

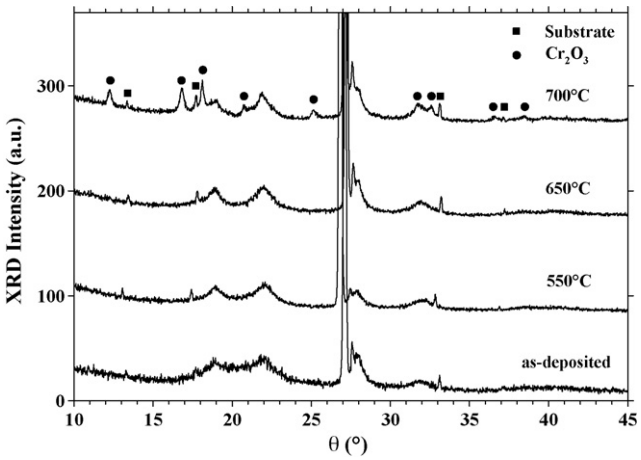

Fig. 5. X-ray diffraction patterns (grazing incidence 2°) of $Cr_3(C_{0.8}N_{0.2})_2$ (350 nm)/SiO_2/Si samples annealed at various temperatures during 30 min under helium atmospheric pressure.

contamination of the reactor. SIMS depth profiles confirm this interpretation.

5. IR pyrometry analysis of the growth mode of an Fe MOCVD process

The third example relates to the monitoring of Fe deposition by MOCVD starting from the gas mixture $FeCp_2$ and H_2O. In this process described elsewhere, the presence of water vapor avoids the nucleation in homogeneous phase and a strong incorporation of carbon into the film [13]. The growth mode is particularly original. Indeed, a very powdered black layer is formed during the first minutes of deposition then, after approximately 10 min, the film transforms very quickly during the deposition (in a few seconds) in order to become a grey and compact metallic film whatever the substrate. Generally, the compact grey layer starts to be formed from the black powdered layer at one edge of the sample and extends across the sample by lateral growth forming the metallic grey layer in few tens of seconds. These visual observations are confirmed by SEM analyses (Fig. 6). In the early stages (time $\leq$ 12 min), the black films are very porous and constituted of spherical, monodisperse and nanometric grains. Then, they rapidly grow to a micrometric size and they form a compact metallic layer. XRD diagrams reveal that the black porous layers are constituted mainly of iron with a small amount of Fe_3C and are strongly contaminated by C and iron oxides (FeO and Fe_3O_4). The quantities of carbon and oxides decrease by increasing the deposition time to become negligible in the dense metallic film obtained after 15 min.

The temporal variation of the pyrometric signal during this process is shown in Fig. 7. The curve is slightly disturbed due to the temperature regulation of the HF generator. In addition to a short period due to the nucleation which increases the surface roughness and thus the emissivity, a first range is observed which is related to the growth of the powdered black layer. Then, an abrupt change of the pyrometric signal is observed before to be stabilized to a characteristic value related to the grey compact layer. In agreement with the XRD analyses, we attribute this evolution of the growth mode to a reduction of the oxides formed in the first stages by the co-deposited carbon. Indeed, according to the Ellingham's diagram the following reactions are expected to occur:

$$\text{at } 640\,^{\circ}\text{C}: \quad 4C + Fe_3O_4 \rightarrow 4CO + 3Fe$$

$$\text{at } 710\,^{\circ}\text{C}: \quad C + FeO \rightarrow CO + Fe$$

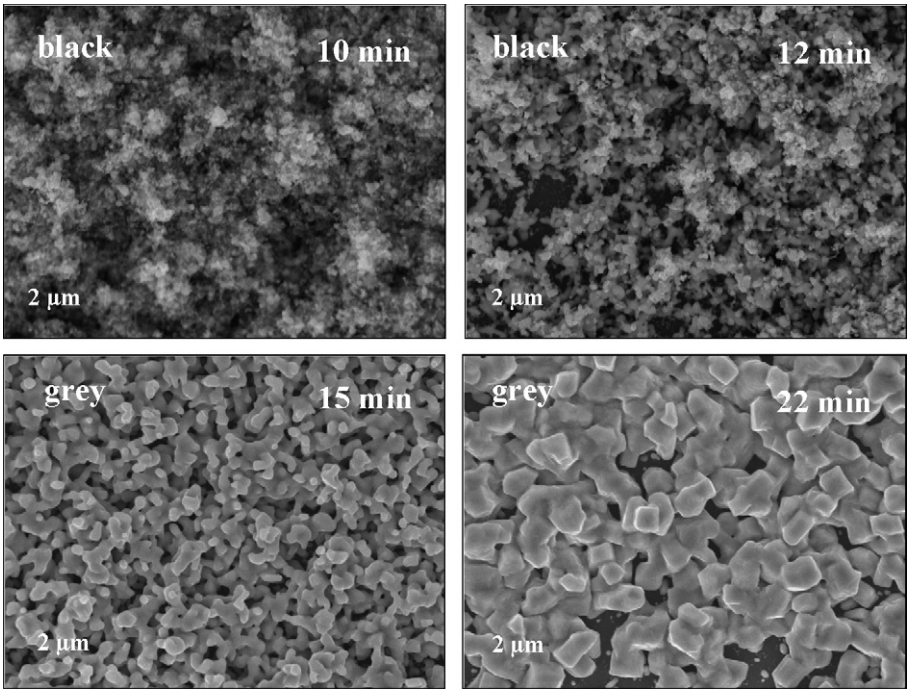

Fig. 6. SEM micrographs of Fe layers obtained starting from $FeCp_2$ and H_2O at 750 °C on Si(1 0 0) under atmospheric pressure for different deposition time ($H_2O/FeCp_2$, molar ratio = 4).

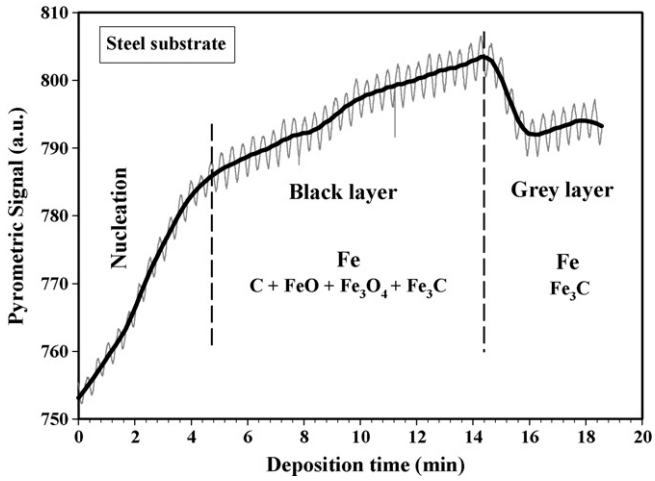

Fig. 7. Variation of the pyrometric signal *vs*. the deposition time during Fe growth at 750 °C on steel substrate starting from the reactive gas mixture $H_2O/FeCp_2$ (molar ratio = 6). The continuous line represents the smoothing of pyrometric signal and the oscillations are due to the temperature regulation. The phases indicated were identified by XRD, Fe being the dominant phase.

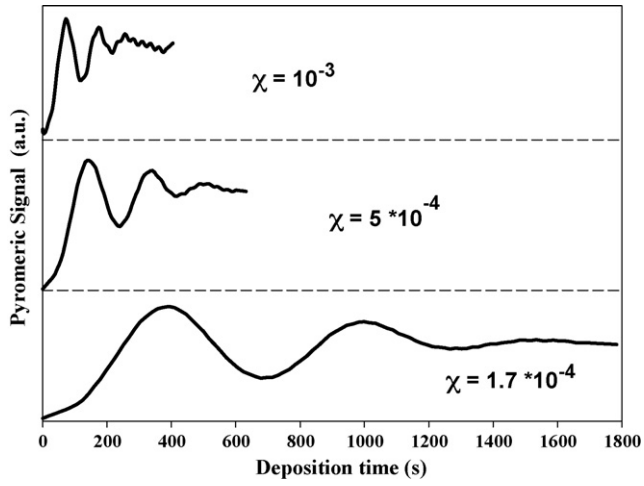

Fig. 8. Variation of the pyrometric signal with the deposition time during three TiO_2 CVD runs carried out at 500 °C on Si(1 0 0) using different mole fractions of $Ti(O^iPr)_4$: 170, 500 and 1000 ppm.

Once these reactions being complete, *i.e*. after approximately 15 min, the compact Fe layer that has been already formed continues to grow and probably exhibit an autocatalytic effect for the process which avoids the formation of oxide and carbon as in the early stages of the run.

6. CVD TiO_2 monitoring by pyrometric interferometry

The last example deals with the use of IR pyrometry as already reported in the literature to monitor the growth of diamond film in a microwaves plasma process [7–9] or the growth of III–V semiconductors by MBE [10,11]. Here, the technique has been used in a CVD process operating under atmospheric pressure for the growth of TiO_2. Two specific growth conditions lead to different characteristics of the TiO_2 layers (they will be called examples 1 and 2 in the following). The radiation emitted by the heated substrate undergoes multiple reflections at the various interfaces (pyrometric interferometry) in good agreement with the phenomena occurring during the conventional spectroscopic analysis in transmission and reflection. The fundamental theoretical details are presented elsewhere [14].

The CVD process was previously described. It uses a similar reactor as for the above examples and it is known that the growth rate of TiO_2 film increases with the molar fraction of $Ti(O^iPr)_4$ used as organometallic source [15]. Fig. 8 shows the temporal variation of pyrometric signal during the growth of TiO_2 using various molar fractions of precursor which means as a function of the growth rate. The pyrometric signal oscillates then damps before to stabilize at a constant value. From this figure, it is obvious that the oscillation period decreases when the deposition rate increases. In fact, as for other spectroscopies, the period P is related to the deposition rate G according to the relation [11]:

$$G = \frac{\lambda}{2nP} \tag{2}$$

where λ is the wavelength of the pyrometer and n the optical index of the film. Consequently, the thickness may be determined *in situ* if the refractive index n is known. Furthermore, the thickness uniformity may be checked in real time in several points of a large sample. A model suggested by Yin shows that the oscillations amplitude depends on the optical index of the film while the damping depends on the roughness [16]. The application of this model to our experimental data does not give entire satisfaction (dotted lines in Fig. 9). We propose to improve this model by taking into account the emissivity of the film during the growth. The detail of this model is reported elsewhere [14]. Here, it suffices to mention that the radiation emitted by the film–substrate system originates both from the substrate through the thin film (as in the example 1 of this paper) and directly from the film considered as a semi-transparent medium and not as a transparent one as in the Yin's model.

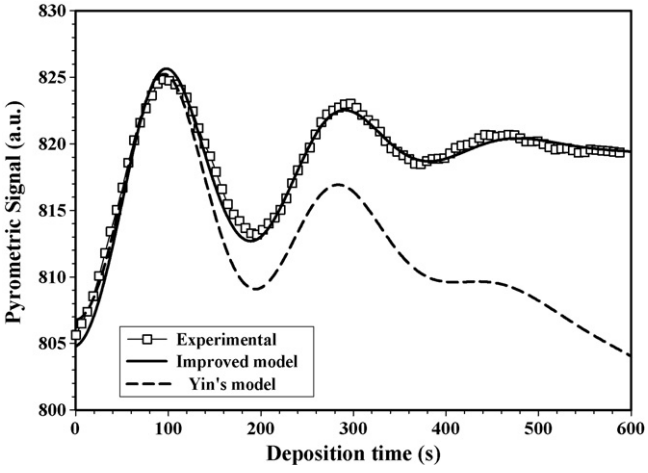

Fig. 9. Experimental and theoretical variations of the pyrometric signal with the deposition time for a TiO_2 CVD run carried out on Si(1 0 0) at 550 °C. The parameters provided by the amended model are: $G = 2.7$ nm/s; $n_{film} = 1.45$; $k_{film} = 0.015$; σ (nm) = 0.4 (t with t = time (s); thickness = 1620 nm (thickness measured by SEM = 1600 nm).

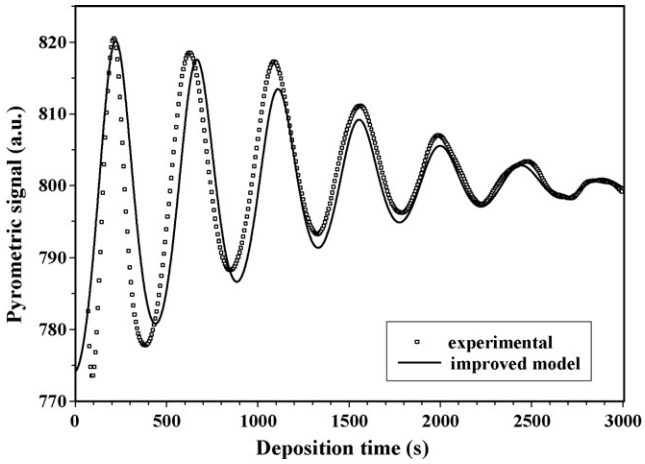

Fig. 10. Experimental (doted line) and theoretical variations (full line) of the pyrometric signal with the deposition time for a run carried out at 500 °C. The parameters provided by the model are: $G = 0.92$ nm/s; $n_{film} = 2$; $k_{film} = 0.0013$; σ_{film} (nm) = 0.035 (t + σ_{subst}, with t = time (s) and $\sigma_{subst} = 40$ nm; thickness = 2760 nm (thickness measured by SEM = 2800 nm).

Fig. 9 shows that this new model (full line) simulates quite well the experimental variation of the pyrometric signal during the growth. *In situ* determination of the growth rate on Si(1 0 0) give a film thickness (1620 nm) in very good agreement with *ex situ* measurement made by SEM (1600 nm). Moreover, the model allows the determination of optical index and roughness values which are however fitting parameters that must be used with precaution (example 1).

TiO_2 films grown under other conditions (example 2) are particularly uniform and denser compared with atmospheric CVD layer of example 1. Fig. 10 shows the pyrometric signal during the growth of TiO_2 at 500 °C on a substrate with a different emissivity. Many oscillations are observed with amplitude significantly higher than for CVD films on Si indicating that these TiO_2 layers have a higher optical index. The agreement between the thickness determined by *in situ* pyrometry IR (2760 nm) and measured *ex situ* by SEM (2800 nm) is very satisfactory. The value of the optical index determined by this method is larger for films of the second series ($n = 2$) compared to those of the first one ($n = 1.35$) in agreement with their difference of porosity.

7. Conclusions

Under certain MOCVD conditions, the formation of an undesired oxidized interphase was *in situ* revealed by IR pyrometry during deposition of CrC_xN_y conducting barriers on Si. It was also possible to determine the nanometric thicknesses of this oxidized underlayer which is not easy to measure by other techniques. Without this interphase, the temporal variation of the pyrometric signal was correlated to the growth rate of these barriers. The determination of deposition rate in the first stages of the growth would be then possible if the absorption coefficient of these original barriers was known. More generally, any surface reaction involving a change of emissivity is detected in real time. Thus, during the heat treatment of the amorphous as-deposited $Cr_3(C,N)_2$ layers, if a surface oxidation occurs, it clearly induces a variation of the pyrometric signal resulting from the difference in emissivity between an oxide and chromium carbonitride.

The pyrometric monitoring of Fe growth by MOCVD under atmospheric pressure starting from the mixture $FeCp_2/H_2O$ revealed an abrupt transition of the radiation intensity due to a rapid change of the growth mode corresponding to the reduction of iron oxides formed in the first stages by the co-deposited carbon.

In the case of transparent TiO_2 films, as reported for other spectroscopies operating in transmission or reflection mode, the pyrometric signal oscillates in the first stages of the growth because of multireflexions at the interfaces. The oscillations period is directly correlated to the growth rate which can thus be calculated *in situ* if the optical index of deposited film is known. The simulation of the oscillations and their damping makes possible the determination at the same time of the thickness and the optical index of the film. The method was applied successfully to TiO_2 films grown by CVD under various conditions.

The originality of these examples shows very promising perspectives of IR pyrometry for the control of CVD processes, in particular those operating under atmospheric pressure (even if it works also under reduced pressure). Indeed, the pyrometric signal is generally independent of the reactor gaseous atmosphere because it operates at a wavelength where usual molecules like CO or H_2O does not absorb. This is a non-invasive and sensitive surface diagnostic tool.

References

[1] C.T. Foxon, Control of MBE, MOMBE and CBE growth using RHEED, Appl. Surf. Sci. 50 (1991) 28–33.
[2] F. Maury, A.M. Gue, N. Viguier, in: M.D. Allendorf, M.T. Swihart, M. Meyyappan (Eds.), Fundamental Gas-Phase and Surface Chemistry of Vapor Phase Deposition II, vol. 13, Electrochemical Society of Proceedings, Washington, DC, 2001, p. 183.
[3] K. Polska, J.-T. Zettler, W. Richter, J. Jönsson, F. Reinhardt, J. Rumberg, M. Pristovsek, M. Zorn, D. Westwood, R.H. Williams, Surface processes before and during growth of GaAs(0 0 1), J. Cryst. Growth 145 (1994) 44–52.
[4] N. Kobayashi, *In situ* monitoring and control of surface processes in metalorganic vapor phase epitaxy by surface photo-absorption, J. Cryst. Growth 145 (1994) 1–11.
[5] N. Sukidi, K.J. Bachmann, V. Narayanan, S. Mahajan, Initial stages of heteroepitaxy of gap on selected silicon surfaces, J. Electrochem. Soc. 146 (1999) 1147–1150.
[6] S. Barrat, P. Pigeat, I. Dieguez, E. Bauer-Grosse, B. Weber, Initial growth phase of diamond thin films observed by thermal emission spectroscopy, Thin Solid Films 304 (1997) 98–105.
[7] S. Barrat, P. Pigeat, I. Dieguez, E. Bauer-Grosse, B. Weber, Observation of spectral and normal emissivity as a method of surface control during the growth of diamond films deposited by a microwave plasma-assisted CVD technique, Thin Solid Films 263 (1995) 127–133.
[8] Z. Yin, Z.L. Akkerman, F.W. Smith, R. Gat, Determination of film growth rate and surface roughness using *in situ* pyrometry, Mater. Res. Soc. Symp. Proc. 441 (1997) 653–658.
[9] K.A. Snail, C.M. Marks, *In situ* diamond growth rate measurement using emission interferometry, Appl. Phys. Lett. 60 (1992) 3135–3137.
[10] K. Biermann, A. Hase, H. Künzel, Optical pyrometry for *in situ* control of MBE growth of $(Al,Ga)As_{1-x}Sb_x$ compounds on InP, J. Cryst. Growth 201/202 (1999) 36–39.
[11] A.J. SpringThorpe, T.P. Humphreys, A. Majeed, W.T. Moore, *In situ* growth rate measurements during molecular beam epitaxy using an optical pyrometer, Appl. Phys. Lett. 55 (1989) 2138–2140.

[12] C. Gasquères, F. Maury, F. Ossola, *In situ* optical pyrometry in the CVD of metallic thin films for real time control of the growth, Chem. Vap. Deposition 9 (2003) 34–39.

[13] F. Senocq, F.-D. Duminica, F. Maury, T. Delsol, C. Vahlas, J. Electrochem. Soc. 153 (2006) G1025–G1031.

[14] F. Maury, F.-D. Duminica, Diagnostic in TCOs CVD processes by IR pyrometry, Thin Solid Film, in press.

[15] F.-D. Duminica, F. Maury, F. Senocq, Atmospheric pressure MOCVD of TiO_2 thin films using various reactive gas mixtures, Surf. Coating Technol. 188–189 (2004) 255–259.

[16] Z. Yin, H.S. Tan, F.W. Smith, Determination of the optical constants of diamond films with a rough growth surface, Diamond Relat. Mater. 5 (1996) 1490–1496.